

Article

Continuity-Aware Scheduling Algorithm for Scalable Video Streaming

Atinat Palawan ^{*}, John C. Woods and Mohammed Ghanbari

School of Computer Science and Electronic Engineering, University of Essex, Colchester, Essex CO4 3SQ, UK; woodjt@essex.ac.uk (J.C.W.); ghan@essex.ac.uk (M.G.)

* Correspondence: apalaw@essex.ac.uk; Tel.: +44-0-1206-872-795

Academic Editor: Pedro Alonso Jordá

Received: 15 February 2016; Accepted: 24 May 2016; Published: 30 May 2016

Abstract: The consumer demand for retrieving and delivering visual content through consumer electronic devices has increased rapidly in recent years. The quality of video in packet networks is susceptible to certain traffic characteristics: average bandwidth availability, loss, delay and delay variation (jitter). This paper presents a scheduling algorithm that modifies the stream of scalable video to combat jitter. The algorithm provides unequal look-ahead by safeguarding the base layer (without the need for overhead) of the scalable video. The results of the experiments show that our scheduling algorithm reduces the number of frames with a violated deadline and significantly improves the continuity of the video stream without compromising the average Y Peak Signal-to-Noise Ratio (PSNR).

Keywords: H.264 SVC; jitter-tolerant scheduling; scalable video streaming; unequal jitter protection

1. Introduction

In recent years, the rise of consumer demand for the distribution and access of video content on packet networks has resulted in the development of a number of commercial offerings. Consumer electronic devices including set top boxes, lap-tops and mobile devices have posed significant challenges to the video-related industry. Competition between service providers has resulted in a number of video standards being launched into the market. Although network capacity has increased rapidly, a commonly encountered problem is bandwidth fluctuation. Indeed, an increase/decrease of bandwidth availability causes jitter or the variation of inter-arrival time between consecutive packets [1–4]. Jitter results in an increase in the number of frames arriving at their destination after play-out time, *i.e.* with a deadline violation. The frames or packets which arrive at their destination after the deadline will not be decoded and consequently, the average quality of the video is degraded [3–5].

Among the various video standards, the Scalable Video Codec (SVC) an extension of the H.264/AVC [6] has been designed to tolerate more adverse network conditions. The sender of scalable video can adjust the bit-rate to correspond to the available bandwidth without re-encoding. This approach has led us from “it works or it does not work” [6] to a more flexible video flow that may be shrunk to suit the available bandwidth. In other words, the primary advantage of scalable video is its elasticity, where the video quality is tailored to the network conditions. In order to shrink a video bit stream, a particular portion of the data; a Network Abstraction Layer (NAL) unit can be removed from the encoded stream prior to delivery to the receiver. In the decoding process, the receiver is able to decode the bit stream if and only if all ancestor NAL units have been received and decoded correctly.

To decode any frame, at least one NAL unit from the base layer is required. For this reason, the base layer is the most important layer from the perspective of continuity and must be preserved.

This paper gives more analysis and discussions to our previous study [7] which addresses the problem of discontinuity of video caused by the late arrival of NAL units. We introduce a novel sender

side scheme which provides unequal jitter protection to a scalable video stream; called the Look Ahead Scheduling Algorithm (LASA). The scheduling algorithm tends to prioritize the base layer but not at the expense of degrading the overall PSNR.

The video stream could be smoothed by using playback buffer management in the receiver but at the expense of real-time interactivity. Our sender side scheme can also collaborate with a receiver based buffer mechanism and provides further improved performance. We exploit the advantages of scalable video by providing unequal look ahead to the SVC video layer.

The rest of this paper is structured as follows. Section 2 is the related work. Our proposed algorithm and related mathematical analysis are presented in Section 3, the simulation results are described in Section 4 and concluding remarks are given in Section 5.

2. Related Work

2.1. Effect of Jitter to Perceptual Video Quality

If there are no variations in delay, the time between two consecutive pieces of data will never change; the flow of video observed at the receiver is as smooth as at the sender side. If jitter is present the time between consecutive packets is unknown prior to delivery. In Internet traffic jitter can be of the order of hundreds of milliseconds which has the potential to distort the video [3].

Figure 1 shows the effects jitter can have on continuity. In the figure the frame arriving after its decoding time will never be displayed. Loss concealment can be applied to repair the distortion but at the expense of reduced video quality. The impact of the continuity on perceived video quality has been investigated in [8,9].

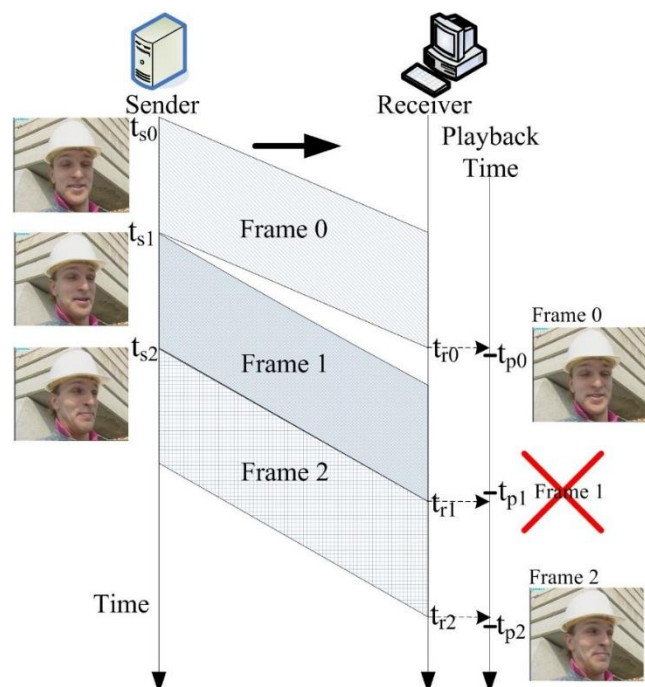


Figure 1. Jitter or variation of delay causes degradation in continuity of a video stream.

As a result of jitter, the perceptual quality is reduced and it has nearly the same effect as packet loss [10].

2.2. Jitter Buffer

The primary mechanism to cope with playback interruption is to create a jitter or playback buffer at the receiver [11,12] where the incoming data are stored temporally before playback. The main

problem with using only playback buffer to cope with bandwidth fluctuation is that in the event of high jitter, the end-to-end delay and playback delay will be high as well [13]. This research proposes a different approach, which is able to support each other boosting immunity to jitter.

2.3. Scalable Video and Its Flexibility

Much work has been done on scalable video and its ability to adapt; either to shrink or stretch to suit the available bandwidth and user preferences [14,15]. In addition to being flexible in unstable network conditions, the SVC is also capable of adjusting according to: the quality of the picture, the bit-rate or even the power limitations of the display device [16]. In [17], the collaborative streams share the same bottleneck link in a home network. Bandwidth probing estimates the available transmission bandwidth and the SVC flow is then adjusted to suit the channel capacity. The study in [18] uses two Transmission Control Protocol (TCP) connections to transmit one scalable video session with one TCP connection dedicated to the base layer and one TCP connection for all the other enhancement layers. Using parallel TCP connections gives more tolerance to congestion and jitter, however, the higher tolerance gives protection to the base and enhancements equally. The research in [19] presents an efficient video adaptation scheme in the Long-Term Evolution (LTE) networks using the distance between user equipment and the LTE base station as a metric to reduce the size of the scalable video stream.

Figure 2 illustrates the idea of packet removal in scalable video. Some of the NAL units can be removed from the video stream by the sender, if bandwidth is scarce. Although in the figure the top layer NAL unit is discarded, the frame is still decodable albeit at lower quality. Packet removal is the primary method to adjust bit-rate in the SVC.

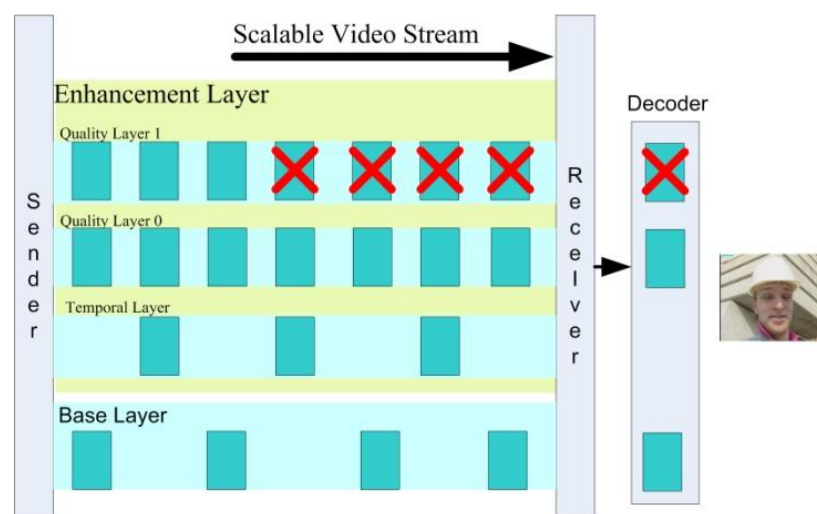


Figure 2. An example of possible Network Abstraction Layer (NAL) unit removal in scalable video.

2.4. Scalable Video Scheduling, Reordering and Packet Selection

Layer-based and frame-based scheduling algorithms are mixed to suite the congestion and jitter level [17]. In the case of high congestion the layer-based scheme will produce better results. If the network is stable, frame-based scheduling is best employed. Alternatively packet selection schemes can be employed to reduce bit-rate, where the objective is to adjust the bit-rate by selecting the best group of packets that minimize the distortion [20–22]. The 3D scalable video scheduling in P2P networks was proposed in [23]. In this study, a client chooses the appropriate layers of scalable video along with a suitable depth according to the limited download bandwidth. The algorithm in this study also provides checking to guarantee the smoothness of the video by considering the playback deadline of each video packet in the base layer. The technique proposed in [24] is used to transmit scalable video

streaming in MC-CDMA. To improve video quality, this study used partial channel state information (PCSI) to give different priorities to each layer of scalable video. The study in [25] proposed a technique using interleaving scheme to prioritize NAL units for real-time MVC video streaming. Other research on packet selection considers the status of the ancestor packets before sending the descendants [26,27]. If an ancestor has not been scheduled, the descendant packet will be discarded. This method reduces the number of the descendant packets that are transmitted but cannot be decoded.

2.5. Unequal Protection

The SVC is a layered video scheme in which the video flow is composed of multiple layers, each with different importance. Unequal error protection can be applied to protect the more important layers using Forward Error Correction (FEC). The research in [28] first applied forward error correction (FEC) to provide prioritization in the network layer rather than more traditional physical layer. FEC is an effective method of protection but adds overhead to the stream. In [5], to increase the quality of video, the researchers give higher priority to the more important layers using Reed-Solomon coding, this is in conjunction with priority-aware block interleaving (PBI) in the MAC layer. The research presented in [29] proposed an unequal recovery algorithm to lost packets which has higher retry transmission rates for the base layer compared to the enhancement layers. However, this algorithm needs a retransmission mechanism to archive the smoothness of video flow.

3. Proposed Algorithm and Its Analysis

We propose a new technique which uses round robin with unequal look ahead scheduling. The Look Ahead Scheduling Algorithm is named as LASA. By setting unequal look-ahead limits to each layer, unequal protection against discontinuity will be achieved. In this algorithm, the base layer is allocated a larger look-ahead limit than the other layers, the probability of a frame with deadline violation is decreased accordingly.

3.1. An Overview of the LASA Scheduling Algorithm

In order to describe LASA scheduling in detail, we compare our algorithm with frame-based and layer-based scheduling. In general, both frame-based and layer-based use traditional round robin scheduling. Frame-based scheduling algorithms schedule all enhancement NAL units which depend on the current base layer NAL unit. In other words, a base layer NAL unit and its enhancement NAL units which represent the same frame will be scheduled consecutively.

In Figure 3, we assume that the scalable video which is composed of a base layer and two enhancement layers has a Group of Pictures (GOP) size of 8. The arrows and numbers show the order of NAL unit scheduling. The notion of a frame-based scheduling algorithm is shown in Figure 3a.

Alternatively, in a layer-based scheduling algorithm, the sending order proceeds along the horizontal axis until the algorithm reaches the upper bound marked by the dark vertical line in Figure 3b, after that the upper layer will be scheduled.

Our LASA scheduling algorithm is shown in Figure 3c. Similar to the layer-based scheduling algorithm, LASA orders the NAL units in the horizontal direction. The unequal bound, which is marked by the dark line, defines the upper bound of NAL units scheduled per layer. In the example shown in Figure 3c, the base layer is allocated with the most look-ahead value, whereas the top layer obtains the least look-ahead value.

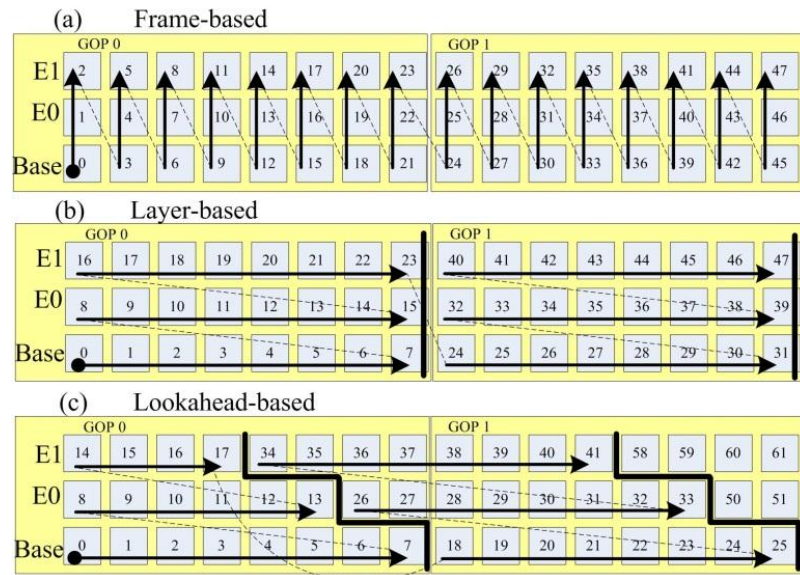


Figure 3. The concept of the three different scheduling schemes discussed. (a) A frame-based scheduling algorithm; (b) A layer-based scheduling algorithm; and (c) The Look Ahead Scheduling Algorithm (LASA) scheduling algorithm.

3.2. LASA Scheduling Algorithm and Its Look-Ahead Limit

In this section, we describe the essential parameters of the LASA scheduling algorithm. In Figure 4, there are two type of parameters *look-ahead* (L_{base} , L_{e1} and L_{e2}) and *deltal_i*.

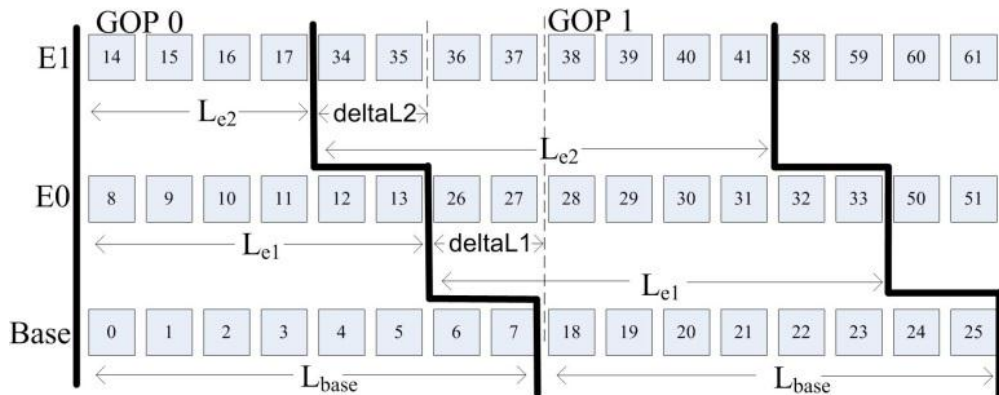


Figure 4. Look-ahead value is allocated to each layer unequally.

L_{base} , L_{e1} and L_{e2} are the look-aheads limit of the base layer, the first enhancement layer and the second enhancement layer, respectively. In the example shown in Figure 4 we assume that the GOP size is 8 and there are 3 layers: base layer, E0, and E1 or layer 0, 1, and 2 respectively. The LASA algorithm starts scheduling at the NAL unit numbered 0 to the NAL unit numbered 7. The value of look-ahead for the base is therefore 8 that is $L_{base} = 7$. For layer E0 and E1, $L_{e1} = 5$ and $L_{e2} = 3$ respectively. DeltaL1 is the difference between layer 0 and layer 1 and deltaL2 is the difference between layer 2 and layer 1. Therefore, deltaL_i is the difference between layer i and i−1. The pseudocode of the LASA scheduling algorithm is shown in Algorithm 1.

We can consider that frame based scheduling is when the parameters are assigned to be deltaL = 0, $L_{base} = 1$, $L_{e1} = 1$ and $L_{e2} = 1$, respectively and layer-base scheduling is when deltaL = 0, $L_{base} \geq 1$,

$L_{e1} \geq 1$ and $L_{e2} \geq 1$ respectively. For LASA, the parameters $\Delta L > 0$, $L_{base} \geq 1$, $L_{e1} \geq 1$ and $L_{e2} \geq 1$, respectively.

Algorithm 1. The pseudocode of the LASA scheduling algorithm.

LASA Algorithm:

Initial Section

- initialize LookAhead of Base layer (0^{th}) to MaxLookAhead
 - initialize LookAhead of Enhancement layer i (i^{th}) to $\text{MaxLookAhead} - \sum_{x=1}^{x=i} \Delta L_x$, where i is top layer.
 - initialize current upper bound of layer i^{th} to LookAhead of layer i^{th}
 - initialize current NAL Unit index of layer i^{th} to 0
-
- Main Section*

While (NOT All Layers Reach End Of Frame Sequence)

For each layer $i = 0^{\text{th}}$ to Top Layer

While (current NAL Unit index of layer i^{th} \leq current upper bound of layer i^{th}
 AND
 current NAL Unit index of layer i^{th} \leq LastFrame
)
 - send current NAL Unit of layer i^{th}
 - Increment current NAL unit index of layer i^{th}
 EndWhile
 - set current upper bound of layer i^{th} to current
 upper bound of i^{th} + LookAhead of layer i^{th}
 - set LookAhead of layer i^{th} to MaxLookAhead
 EndFor
EndWhile

3.3. An Analysis of the LASA Scheduling Algorithm

Mathematical Analysis

This section is dedicated to the analysis of the LASA algorithm in which we show that the sending time for NAL units in the base layer, scheduled by LASA have sending times less or equal to layer-based scheduling.

We define the following terms:

$t_{lay_{[g,l,i]}}^s$ is the time when layer-based scheduling starts sending a NAL unit g, l, i where g is a group of pictures number, $g \in I$, $g \geq 0$

l is the layer number, $l \in I$, $0 \leq l \leq l_{max}$

i is the sending order of frames, $i \in I$, $0 \leq i \leq gs$.

$t_{lh_{[g,l,i]}}^s$ is the time when LASA starts sending the first bit of the NAL unit g, l, i

$t_{[g,l,i]}^p$ is the time spent between the beginning of the first bit and the end of a NAL unit g, l, i
 l_{max} is the number of layers, so $l_{max} \geq 0$

gs is GOP size, so $gs \geq 1$

Figure 5 shows the meaning of $t_{[g,l,i]}^s$ and $t_{[g,l,i]}^p$.

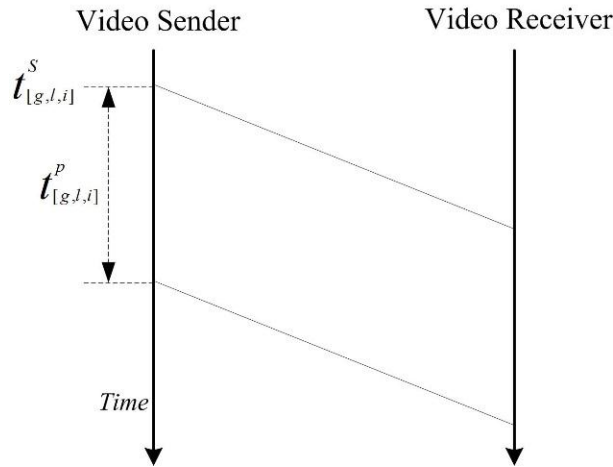


Figure 5. Definition of the time to start sending ($t_{[g,l,i]}^s$) and time spent for sending each NAL unit ($t_{[g,l,i]}^p$) used in this section.

The time to start sending any base layer NAL unit is given in Equation (1).

$$t_{lay_{[x,0,z]}}^s = \sum_{g=0}^{x-1} \sum_{l=0}^{l_{\max}} \sum_{i=0}^{g_s-1} t_{[g,l,i]}^p + \sum_{i=0}^{z-1} t_{[x,0,i]}^p \quad (1)$$

where $x, z \in I$ and $x \geq 1, z \geq 1$.

$$t_{lh_{[x,0,z]}}^s = t_{lay_{[x,0,z]}}^s - t_{skip}^p \quad (2)$$

where t_{skip}^p is the time spent for some NAL units in layer-based scheduling but is not used by LASA scheduling. $t_{skip}^p > 0$ when DeltaL1 or DeltaL2 > 0 as shown in Figure 6b,c.

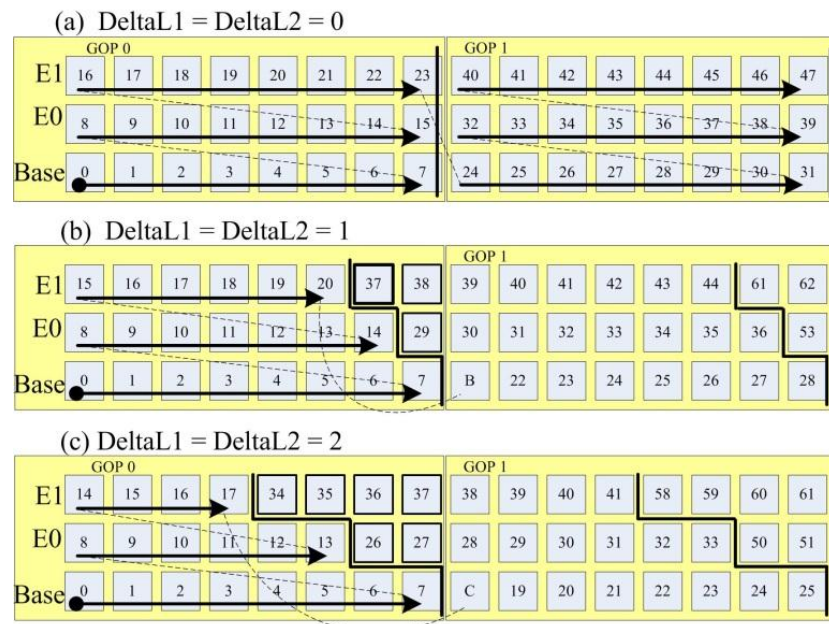


Figure 6. The values of t_{skip}^p when (a) $\text{DeltaL1} = \text{DeltaL2} = 0$ and $t_{skip}^p = 0$; (b) $\text{DeltaL1} = \text{DeltaL2} = 1$ and $t_{skip}^p = t_{29}^p + t_{37}^p + t_{38}^p$; (c) $\text{DeltaL1} = \text{DeltaL2} = 2$ and $t_{skip}^p = t_{26}^p + t_{27}^p + t_{34}^p + t_{35}^p + t_{36}^p + t_{37}^p$.

In Figure 6b, the time spent sending the NAL unit numbers 29, 37 and 38 is t_{skip}^p of Equation (2) when DeltaL1 = DeltaL2 = 1. So, if we use LASA, the NAL unit marked by B, which would otherwise be numbered 21, will be sent earlier than scheduled by the layer-based approach, as shown in Equation (3).

$$t_{lh_B}^s < t_{lay_B}^s \quad (3)$$

where:

$t_{lh_B}^s$ is the time when LASA starts sending NAL unit B.

$t_{lay_B}^s$ is the time when the layer-based scheduling algorithm starts sending NAL unit B.

t_{29}^p, t_{37}^p and t_{38}^p are the times spent for sending NAL units 29, 37 and 38, respectively.

In Figure 6c, the time spent sending the NAL units 26, 27, 34, 35, 36 and 37 is t_{skip}^p when DeltaL1 = DeltaL = 2. Therefore, if the NAL unit marked by C is scheduled by LASA, it will be sent earlier than by layer-based scheduling as shown in Equation (4).

$$t_{lh_C}^s < t_{lay_C}^s \quad (4)$$

With reference to Equation (5), due to $t_{skip}^p > 0$, every NAL unit of the base layer which is scheduled by LASA will be sent earlier than the corresponding layer-based scheduling algorithm.

$$t_{lh_{[x,0,z]}}^s < t_{lay_{[x,0,z]}}^s \quad (5)$$

In the case of the first GOP where $t_{skip}^p = 0$, LASA has not skipped any NAL units. Therefore, in this case, we have

$$t_{lh_{[x,0,z]}}^s = t_{lay_{[x,0,z]}}^s \quad (6)$$

Referring to Equations (5) and (6), we can conclude that the starting time of any base layer NAL unit transmitted by LASA is less than or equal to that of the layer-based scheduling algorithm. The “sooner the better” approach for scheduling the base layer adopted by LASA is the reason the algorithm is able to provide more jitter protection to the base layer. In unpredictable traffic conditions, it is better if base layer NALs have as much time as possible to allow for the unpredictable delay.

Therefore, the result of comparing LASA scheduling and layer scheduling algorithms with respect to sending time is shown in Equation (7).

$$t_{lh_{[x,0,z]}}^s \leq t_{lay_{[x,0,z]}}^s \quad (7)$$

Next, layer-based and frame-based scheduling algorithms are analyzed.

$$\begin{aligned} t_{frm_{[x,0,z]}}^s = & \sum_{g=0}^{x-1} \sum_{i=0}^{gs-1} \sum_{l=0}^{l_{\max}} t_{[g,l,i]}^p + \sum_{i=0}^{z-1} t_{[x,0,i]}^p + \\ & \sum_{i=0}^{z-1} t_{[x,1,i]}^p + \sum_{i=0}^{z-1} t_{[x,2,i]}^p \end{aligned} \quad (8)$$

With reference to Equations (1) and (8), note that, the first and the second terms of Equations (1) are (8). Therefore

$$t_{frm_{[x,0,z]}}^s = t_{lay_{[x,0,z]}}^s + \sum_{i=0}^{z-1} t_{[x,1,i]}^p + \sum_{i=0}^{z-1} t_{[x,2,i]}^p \quad (9)$$

Because of $\sum_{i=0}^{z-1} t_{[x,1,i]}^p \geq 0$ and $\sum_{i=0}^{z-1} t_{[x,2,i]}^p \geq 0$, so we obtain

$$t_{frm_{[x,0,z]}}^s \geq t_{lay_{[x,0,z]}}^s \quad (10)$$

From Equations (7) and (10), we conclude that the base layer NAL unit will receive greater benefit using LASA scheduling than layer-based and frame-based scheduling with respect to the start time of transmission. The order of the starting times for the three different scheduling algorithms is shown in Equation (11).

$$t_{lh_{[x,0,z]}}^s \leq t_{lay_{[x,0,z]}}^s \leq t_{frm_{[x,0,z]}}^s \quad (11)$$

In the next section, the performance of the LASA scheduling algorithm will be evaluated through simulation.

4. Simulation Results

This section is dedicated to the simulation of the LASA scheduling algorithm. The simulation is conducted in a rapidly fluctuating jitter-prone scenario using the network simulator (NS3).

4.1. Simulation Setup

Figure 7 depicts the dumbbell topology constructed for the simulation. Two pairs of end nodes are connected together and share a bottleneck link. All link capacities are set to 2.2 Mb/s and 20 ms for transmission delay. In order to generate rapidly fluctuating bandwidths, an ON/OFF UDP flow with an exponential random variable has been used for the background traffic. The mean ON time period is varied from 0.0 to 0.4 s. The mean OFF period is 1s and the mean UDP packet is set to 1000 bytes.

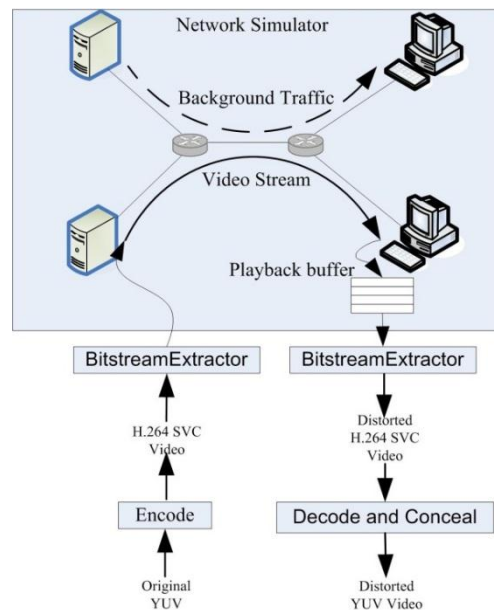


Figure 7. Network topology and input/output video stream used in this simulation.

We concatenated five public frame sequences which are city, foreman, mobile, soccer and harbor. All video clips are 30 fps, 300 frames and CIF (352×288) resolution. This concatenated video is encoded with average bitrate of 1541 kbps by the JSVM reference software [30] and is injected into the NS3 simulator. In the decoding process, the Open SVC Decoder is employed [31,32]. The encoded video is composed of a base layer and two enhancement layers. We use a GOP of 16 frames. In each simulation run, we inject the bit-stream of the concatenated video to the network simulator by setting 60 s of simulation time for each run. We also repeat our simulation with different seeds for the random variable in order to vary the background traffic pattern.

All three scheduling algorithms (LASA, layer-based, and frame-based) were implemented and compared. In the same way as other streaming video research, the buffer has also been added as part

of the simulation to collect NAL units. When pre-buffering threshold is reached, the receiver will start decoding and playout [13].

In the playback buffer management module, it also stamps the receiving time of each NAL unit. If some NAL units arrive at the receiver later than their deadlines, those NAL units will be marked as deadline violations which will not be passed to the decoder. We collected the receiving time of each NAL unit to analyze the number of frames that miss their deadlines.

All undecodable frames either the missed deadline frames, lost frames or erroneous frames will be concealed with the previous frame in order to maintain the number of frames in the video sequence. In line with other researchers [33] we compare Y PSNR between the original YUV and distorted YUV as shown in Figure 7.

4.2. Performance Evaluation

In this experiment, we compare the performance of the three algorithms by concentrating on the continuity and the average Y PSNR. The result of LASA scheduling reveals that the number of frames that miss the deadline and the number of concealed frames is lower than the layer-based and frame-based scheduling algorithms. LASA scheduling with deltaL equal to 2, 4 or 8 is able to improve results but for deltaL equal to 16 the average Y-PSNR is very similar to layer-based scheduling, but higher than the frame-based method.

The essential parameters are varied. Firstly, the ON time period of background traffic is varied between 0.0 to 0.4 s to produce jitter. Secondly, we vary the pre-buffering threshold of the playback buffer. The larger is the playback buffer the better it is in terms of its ability to resist jitter. We, therefore, vary the period of time before beginning playback from 400 to 600 ms.

In Figures 8–10 the percentages of missed deadlines among the three algorithms are observed.

In Figure 8, the playback buffer threshold is set to 600 ms, the percentage of missed deadline frames for LASA scheduling is lower than layer-based scheduling. LASA scheduling is able to reduce the number of frames missing the deadline considerably. For the case of LASA with deltaL equal to 16, when high burst duration (0.2 to 0.4) is injected, the percentage of missed deadline frames is 0.84% lower than layer-based scheduling on average.

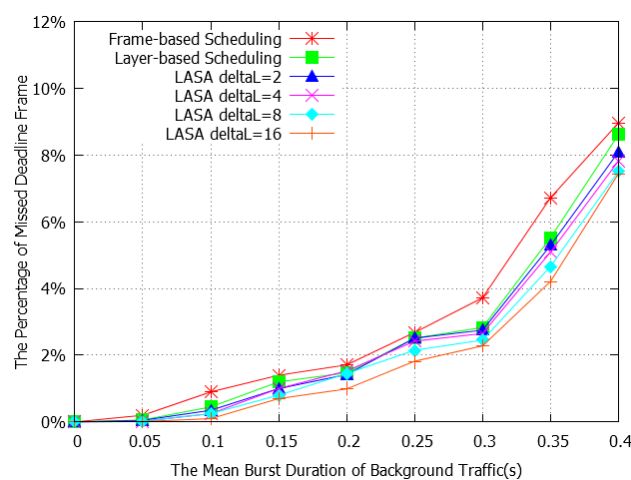


Figure 8. The number of frames with deadline violation when the threshold is 600 ms.

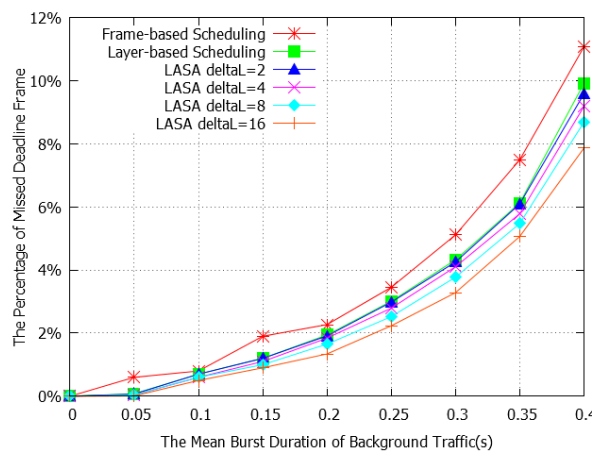


Figure 9. The number of frames with deadline violation when the threshold is 500 ms.

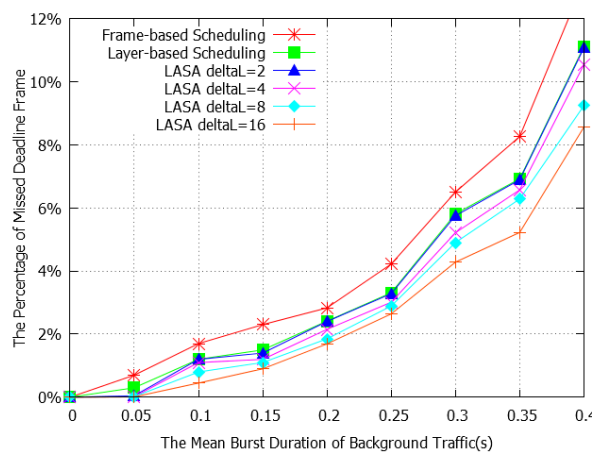


Figure 10. The number of frames with deadline violation when the threshold is 400 ms.

To increase the influence of jitter we reduced the play out buffer from 600 to 500 ms and 400 ms as shown in Figures 9 and 10. As summarized in Table 1, the largest improvement provided by LASA is when $\text{deltaL} = 16$; around 1.43%. When deltaL are 2, 4 or 8, the percentage of missed deadlines are still lower than the layer-based approach. The negative values seen in Table 1 are representative of when LASA is providing improved results over layer-based scheduling.

Table 1. Comparison of the percentage of missed deadline frames between layer-based and the LASA scheduling algorithm when burst duration is varied from 0.2 to 0.4 s.

Threshold	$\text{deltaL} = 2$	$\text{deltaL} = 4$	$\text{deltaL} = 8$	$\text{deltaL} = 16$
400 ms	-0.03	-0.42	-0.88	-1.43
500 ms	-0.01	-0.32	-0.64	-1.11
600 ms	-0.18	-0.29	-0.54	-0.84
Average	-0.07	-0.34	-0.69	-1.13

LASA scheduling has the highest performance of the three scheduling algorithms with respect to the number of frames that have arrived at the receiver after the deadline for playback. The results for buffer thresholds of 600, 500, and 400 ms as shown in Figures 8–10 respectively. These results agree with the mathematical analysis in Equation (11) and our assumption that if we send important NAL units earlier, there is more time to overcome unpredictable delays, and the probability of missing the deadline will be reduced accordingly.

As some base layer NAL units may miss their decoding deadline, or being lost or are in errors, they cause some descendant NAL units not to be decoded even if they arrive at the receiver before the deadline. All undecodable frames will be concealed with their previous frames. The percentages of the undecodable frames are shown in Figures 11–13. From the user’s perspective, if the number of frozen frames increases, the continuity of the video stream decreases.

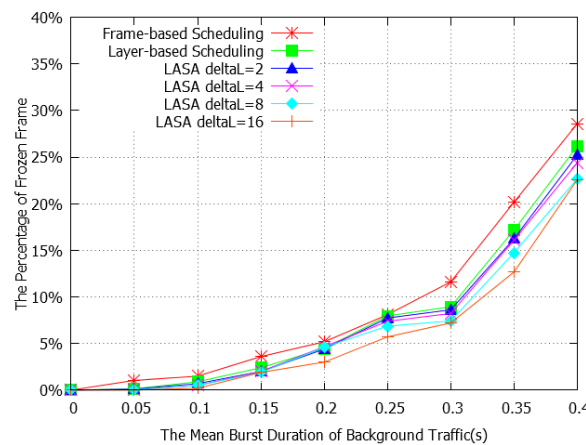


Figure 11. The number of frozen frames when threshold is 600 ms.

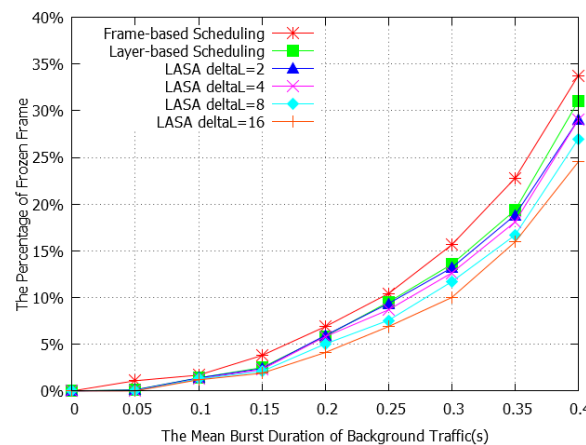


Figure 12. The number of frozen frames when threshold is 500 ms.

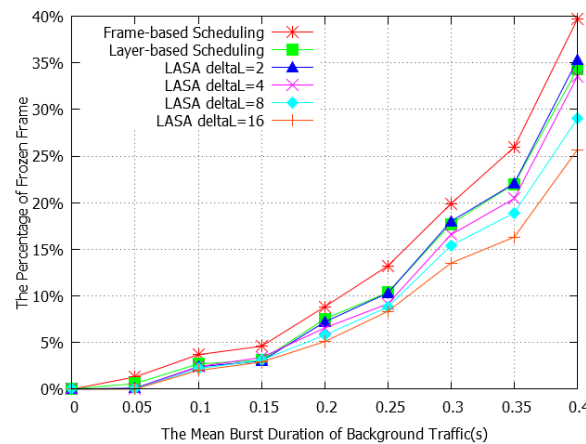


Figure 13. The number of frozen frames when threshold is 400 ms.

In Figure 11, the percentage of frozen frames for LASA scheduling is lower than layer-based and frame-based scheduling. For example, on high burst duration (0.2–0.4 s) LASA with $\text{deltaL} = 16$ is lower than layer-based scheduling by 2.71%. For thresholds of 500 ms, and 400 ms as shown in Figures 12 and 13 the percentages of frozen frames for LASA are lower than layer-based by 3.56% and 4.60% respectively. In Table 2, we compare the percentage of frozen frames between layer-based and LASA. The negative value corresponds to when LASA is better than layer-based in terms of frozen frames.

Table 2. Comparison of the percentage of frozen frames between layer-based and the LASA scheduling algorithm when burst duration is varied from 0.2 to 0.4 s.

Threshold	$\text{deltaL} = 2$	$\text{deltaL} = 4$	$\text{deltaL} = 8$	$\text{deltaL} = 16$
400 ms	0.18	-1.14	-2.81	-4.60
500 ms	-0.59	-1.01	-2.27	-3.56
600 ms	-0.50	-0.80	-1.69	-2.71
Average	-0.30	-0.98	-2.25	-3.63

LASA scheduling is designed to give more protection to the base layer by sacrificing enhancement layer protection. However, since the loss of base layer data is more damaging than the loss of enhancement data, the overall video quality may not be degraded that much. Moreover, in the LASA algorithm even if we lose video quality in some frames but we gain video continuity by reducing the percentage of frozen frames compared to other rival algorithms. Hence the overall video quality is improved.

Figures 14–16 show that LASA scheduling with deltaL equal to 8 either for 400 ms, 500 ms or 600 ms thresholds is able to improve the Y PSNR significantly by 0.92 dB, 0.96 dB and 0.69 dB, respectively. For LASA scheduling with deltaL equals to 4, Y PSNR is improved by 0.44 dB, 0.43 dB and 0.37 dB. However, in the case of $\text{deltaL} = 2$ and $\text{deltaL} = 16$ the average Y PSNR is similar to layer-based scheduling. In Table 3, we summarize the average Y PSNR of LASA and layer-based scheduling. It should be noticed that, both LASA and layer-based scheduling are better than frame-based.

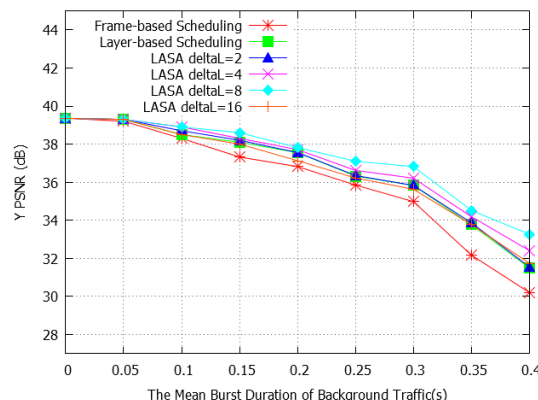


Figure 14. The average Y Peak Signal-to-Noise Ratio (PSNR) when the threshold of the playback buffer is 400 ms.

Table 3. Comparison of Average Y PSNR, in dB, between Layer-based and LASA scheduling algorithms when burst duration is varied from 0.2 to 0.4 s.

Threshold	$\text{deltaL} = 2$	$\text{deltaL} = 4$	$\text{deltaL} = 8$	$\text{deltaL} = 16$
400 ms	0.04	0.44	0.92	-0.09
500 ms	0.04	0.43	0.96	-0.09
600 ms	0.06	0.37	0.69	-0.09
Average	0.05	0.41	0.86	-0.09

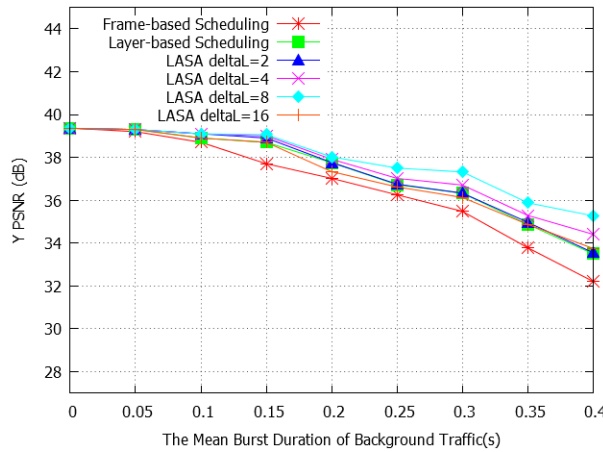


Figure 15. The average Y PSNR when the threshold of the playback buffer is 500 ms.

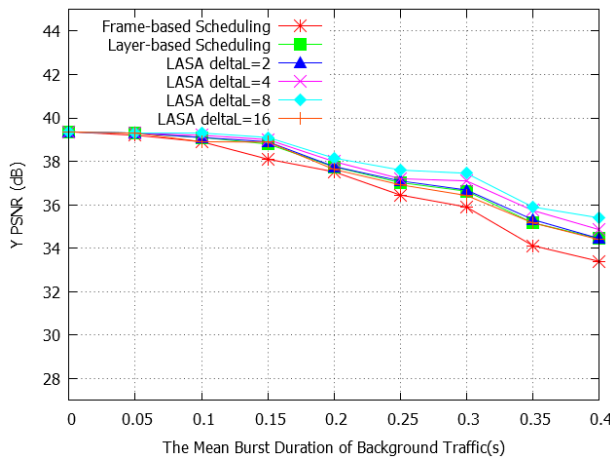


Figure 16. The average Y PSNR when the threshold of the playback buffer is 600 ms.

In Table 3, negative values represent when LASA has a lower PSNR than layer-based scheduling whilst a positive value represents higher. The difference of the average Y PSNR of LASA and layer-based scheduling vary between -0.09 dB to 0.96 dB and it is only when deltaL is equal to 16 that a negative value is obtained.

Due to the parameter deltaL of LASA, sending enhancement layer NAL units can incur delays. To enable the receiver to play the video at the highest quality layer, the per-buffering time setting should exceed the time value t in (12).

$$t = \frac{\sum_{i=0}^{Top-1} (\text{deltaL} * (Top - i))(\frac{Br_i}{Fr_i})}{\text{AverageBandwidth}} \quad (12)$$

where t is pre-buffering time, Br_i is average bitrate of layer i , Fr_i is frame rate of layer i and Top is the top available layer.

5. Conclusions and Discussion

The main contribution of the LASA scheduling algorithm, presented in this paper, is improved continuity of a video stream in a jitter-prone environment by providing an unequal look-ahead value to each layer of a scalable video. It is able to maintain or improve the average Y PSNR compared to layer-based and frame-based scheduling algorithms. In addition to the PSNR improvement of

LASA by up to 4 dB, the continuity of the video is also improved. This quality measurement can be more significant subjectively, as at high video qualities, 4 dB improvement may not be appreciated, but continuity is notable.

By exploiting the flexibility of the scalable video architecture in which a video is composed of one or more layers of unequal importance, improvements in dropped frames and PSNR are demonstrated. With predefined unequal look-ahead values, the base layer scheduled by LASA provides improved safety to the base layer and means the enhancement NAL units do not get discarded.

In addition, the novel approach for jitter resistance of LASA can be integrated with standard playback buffers to improve performance further, if higher end-to-end delay is permissible.

Acknowledgments: We would like to acknowledge the Thai Government for sponsorship and the assistance of staff and students at Essex University UK.

Author Contributions: Atinat Palawan as the main author is responsible for the conception and first realization of the LASA algorithm and demonstration of its advantages. John C. Woods as the principal supervisor provided the background for quantification and verification of video quality and was a major contributor to the documentation. Mohammed Ghanbari as co-supervisor and one of the founders of layered coding was an inspiration for the difficulties encountered when networking layered video.

Conflicts of Interest: The authors declare no conflict of interest.

Abbreviations

The following abbreviations are used in this manuscript:

LASA	Look Ahead Scheduling Algorithm
NAL	Network Abstraction Layer
SVC	Scalable Video Coding
PSNR	Peak Signal-to-Noise Ratio
FEC	Forward Error Correction

References

1. ITU-T. Analysis, Measurement and Modelling of Jitter. In *ITU-T Delayed Contribution COM 12—D98*; ITU-T: Geneva, Switzerland, 2003.
2. Bertsekas, D.; Gallager, R. *Data Networks*, 2nd ed.; Prentice-Hall, Inc.: Upper Saddle River, NJ, USA, 1992; p. 556.
3. Venkataraman, M.; Chatterjee, M. Quantifying video-qoe degradations of internet links. *IEEE/ACM Trans. Netw.* **2012**, *20*, 396–407. [[CrossRef](#)]
4. ITU-T. Perceptual Video Quality Measurement Techniques for Digital Cable Television in the Presence of a Reduced Reference. In *Recommendation ITU-T J.249*; ITU-T: Geneva, Switzerland, 2010.
5. Kyungtae, K.; Jeon, W.J. Differentiated protection of video layers to improve perceived quality. *IEEE Trans. Mob. Computing* **2012**, *11*, 292–304. [[CrossRef](#)]
6. Schwarz, H.; Marpe, D.; Wiegand, T. Overview of the scalable video coding extension of the h.264/avc standard. *IEEE Trans. Circuits Syst. Video Technol.* **2007**, *17*, 1103–1120. [[CrossRef](#)]
7. Palawan, A.; Woods, J.; Ghanbari, M. A jitter-tolerant scheduling algorithm to improve continuity in scalable video streaming. In Proceedings of the 2015 7th Computer Science and Electronic Engineering Conference (CEEC), Colchester, UK, 24–25 September 2015.
8. Huynh-Thu, Q.; Ghanbari, M. Impact of jitter and jerkiness on perceived video quality. In Proceedings of the Workshop on Video Processing and Quality Metrics, Scottsdale, AZ, USA, 1–4 January 2006.
9. Huynh-Thu, Q.; Ghanbari, M. Temporal aspect of perceived quality in mobile video broadcasting. *IEEE Trans. Broadcast.* **2008**, *54*, 641–651. [[CrossRef](#)]
10. Claypool, M.; Tanner, J. The effects of jitter on the perceptual quality of video. In Proceedings of the seventh ACM international conference on Multimedia (Part 2), Orlando, FL, USA, 30 October 1999; pp. 115–118.
11. Su, Y.-F.; Yang, Y.-H.; Lu, M.-T.; Chen, H.H. Smooth control of adaptive media playout for video streaming. *Trans. Multi.* **2009**, *11*, 1331–1339.
12. Kalman, M.; Steinbach, E.; Girod, B. Adaptive media playout for low-delay video streaming over error-prone channels. *IEEE Trans. Circuits Syst. Video Technol.* **2004**, *14*, 841–851. [[CrossRef](#)]

13. Liang, G.; Liang, B. Balancing interruption frequency and buffering penalties in vbr video streaming. In Proceedings of the 2007 26th IEEE International Conference on Computer Communications, IEEE INFOCOM, Anchorage, AK, USA, 6–12 May 2007; pp. 1406–1414.
14. Choi, H.; Kang, J.; Kim, J.-G. Dynamic and interoperable adaptation of SVC for QoS-enabled streaming. *IEEE Trans. Consum. Electron.* **2007**, *53*, 384–389. [[CrossRef](#)]
15. Wien, M.; Cazoulat, R.; Graffunder, A.; Hutter, A.; Amon, P. Real-time system for adaptive video streaming based on SVC. *IEEE Trans. Circuits Syst. Video Technol.* **2007**, *17*, 1227–1237. [[CrossRef](#)]
16. Lee, H.; Lee, Y.; Lee, J.; Lee, D.; Shin, H. Design of a mobile video streaming system using adaptive spatial resolution control. *IEEE Trans. Consum. Electron.* **2009**, *55*, 1682–1689. [[CrossRef](#)]
17. Kim, D.; Chung, K. A network-aware quality adaptation scheme for device collaboration service in home networks. *IEEE Trans. Consum. Electron.* **2012**, *58*, 374–381. [[CrossRef](#)]
18. Chaurasia, A.K.; Jagannatham, A.K. Dynamic parallel tcp for scalable video streaming over mimo wireless networks. In Proceedings of the 2013 6th Joint IFIP, Wireless and Mobile Networking Conference (WMNC), Dubai, United Arab Emirates, 23–25 April 2013; pp. 1–6.
19. Radhakrishnan, R.; Nayak, A. An efficient video adaptation scheme for svc transport over lte networks. In Proceedings of the 2011 IEEE 17th International Conference on Parallel and Distributed Systems (ICPADS), Tainan, Taiwan, 7–9 December 2011; pp. 127–133.
20. Maani, E.; Yijing, L.; Pahalawatta, P.; Katsaggelos, A. Packet scheduling for scalable video streaming over lossy packet access networks. In Proceedings of 16th International Conference on Computer Communications and Networks, 2007, ICCCN 2007, Honolulu, HI, USA, 13–16 August 2007; pp. 591–596.
21. Miao, Z.; Ortega, A. Optimal scheduling for streaming of scalable media. In Proceedings of the 2000 Conference Record of the Thirty-Fourth Asilomar Conference on Signals, Systems and Computers, Pacific Grove, CA, USA, 29 October–1 November 2000; Volume 1352, pp. 1357–1362.
22. Chou, P.A.; Zhourong, M. Rate-distortion optimized streaming of packetized media. *IEEE Trans. Multimedia* **2006**, *8*, 390–404. [[CrossRef](#)]
23. Liu, Y.; Liu, J.; Song, J.; Argyriou, A. Scalable 3d video streaming over p2p networks with playback length changeable chunk segmentation. *J. Visual Commun. Image Represent.* **2015**, *31*, 41–53. [[CrossRef](#)]
24. Seo, H.; Lee, K. Effective scalable video streaming transmission with TBS algorithm in an MC-CDMA system. *Inf. Syst.* **2015**, *48*, 313–319. [[CrossRef](#)]
25. Liu, Z.; Qiao, Y.; Karunakar, A.K.; Lee, B.; Fallon, E.; Zhang, C.; Zhang, S. H. 264/mvc interleaving for real-time multiview video streaming. *J. Real-Time Image Process.* **2015**, *10*, 501–511. [[CrossRef](#)]
26. Jurca, D.; Frossard, P. Video packet selection and scheduling for multipath streaming. *IEEE Trans. Multimedia* **2007**, *9*, 629–641. [[CrossRef](#)]
27. De Vleeschouwer, C.; Frossard, P. Dependent packet transmission policies in rate-distortion optimized media scheduling. *IEEE Trans. Multimedia* **2007**, *9*, 1241–1258. [[CrossRef](#)]
28. Hellge, C.; Gomez-Barquero, D.; Schierl, T.; Wiegand, T. Layer-aware forward error correction for mobile broadcast of layered media. *IEEE Trans. Multimedia* **2011**, *13*, 551–562. [[CrossRef](#)]
29. Kuo, W.H.; Kaliski, R.; Wei, H.Y. A qoe-based link adaptation scheme for H.264/SVC video multicast over IEEE 802.11. *IEEE Trans. Circuits Syst. Video Technol.* **2015**, *25*, 812–826. [[CrossRef](#)]
30. JVT. Iso/iec 14496–10 amd.3 Scalable Video Coding. In Doc. JVT-X201; ITU-T: Geneva, Switzerland, 2007.
31. Blestel, M.; Raulet, M. Open SVC decoder: A flexible SVC library. In Proceedings of the international conference on Multimedia, Firenze, Italy, 8–10 October 2010; pp. 1463–1466.
32. Pescador, F.; Samper, D.; Raulet, M.; Juarez, E.; Sanz, C. A DSP based H.264/SVC decoder for a multimedia terminal. In Proceedings of the 2011 IEEE International Conference on Consumer Electronics (ICCE), Las Vegas, NV, USA, 9–12 January 2011; pp. 401–402.
33. Cho, Y.; Kwon, D.K.; Liu, J.; Kuo, C.J. Dependent r/d modeling techniques and joint t-q layer bit allocation for H.264/SVC. *IEEE Trans. Circuits Syst. Video Technol.* **2013**, *23*, 1003–1015. [[CrossRef](#)]

